Available online at www.sciencedirect.com
ScienceDirect
Ceramics International 36 (2010) 1365–1372
CERAMICS INTERNATIONAL
www.elsevier.com/locate/ceramint

Synthesis and characterization of multiferroic $BiFeO_3$ powders fabricated by hydrothermal method

Seung Ho Han [a,b], Kyoung Sun Kim [a], Ho Gi Kim [a], Hyeung-Gyu Lee [b], Hyung-Won Kang [b], Jeong Seog Kim [c], Chae Il Cheon [c,*]

[a] Department of Materials Science and Engineering, Korea Advanced Institute of Science and Technology, Daejeon 305-701, Republic of Korea
[b] Electronic Materials and Device Research Center, Korea Electronics Technology Institute, Seongnam, Gyeonggi 463-816, Republic of Korea
[c] Department of Semiconductor and Display Engineering, Hoseo University, Asan, Chungnam 336-795, Republic of Korea

Received 17 July 2009; received in revised form 9 October 2009; accepted 7 January 2010
Available online 29 January 2010

Abstract

The influence of processing parameters on phase formation and particle size of hydrothermally synthesized $BiFeO_3$ powders was investigated. $BiFeO_3$ powder was synthesized by dissolving bismuth nitrate and iron nitrate in KOH solution at temperatures ranging from 150 to 225 °C. X-ray diffraction patterns and scanning electron microscopy observation indicated that rod-like α-Bi_2O_3 phase was formed at initial stage of reaction and dissolved into ions to form thermodynamically stable $BiFeO_3$ phase. Single-phase perovskite $BiFeO_3$ has been formed using a KOH concentration of 8 M at a temperature of ≥175 °C in a 6 h reaction period. $BiFeO_3$ particle growth was promoted by lowering the KOH concentration, or increasing the duration time or reaction temperature. The effects of processing conditions on the formation of crystalline $BiFeO_3$ powders were discussed in terms of a dissolution–precipitation mechanism. The magnetization of the $BiFeO_3$ powders at room temperature showed a weak a ferromagnetic nature.

Keywords: A. Powders: chemical preparation; B. Electron microscopy; B. X-ray methods; C. Magnetic properties

1. Introduction

Multiferroic materials, which show both ferroelectric and ferromagnetic properties in a certain temperature range, have attracted considerable attention due to the fascinating fundamental physics underlying their behavior and potential applications for novel magnetoelectric devices [1–3]. Of particular interest is $BiFeO_3$ (BFO), which exhibits ferroelectric and antiferromagnetic properties at room temperature. Its phase transition temperatures are high ($T_N = 370$ °C and $T_C = 810$ °C), making it very attractive from an application point of view [4,5]. In addition to potential magnetoelectric applications, BFO might find applications in optoelectronic devices [6] and gas sensing materials [7] due to its small bandgap and gas sensitivity, respectively.

Perovskite BFO is usually fabricated by a conventional solid-state reaction at a high sintering temperature [8]. Other fabrication methods also require a high temperature treatment during or after the synthesis. As such, it is difficult to obtain single-phase materials, because the volatilization of some reactants leads to an incomplete reaction. Recently, researchers have attempted to prepare phase pure BFO via a variety of routes, including rapid thermal annealing [9,10], sol–gel method [11,12] and hydrothermal method [13–17]. Among these fabrication techniques, hydrothermal approaches to obtain phase pure BFO powders warrant further investigation, because the synthesis of crystalline ceramics is possible by hydrothermal reaction at a temperature of 200 °C or lower without a further calcination step. In the case of BFO, such low processing temperatures prevent the volatilization of reactants and minimize the amount of impurities associated with calcinations and ball-milling steps. BFO powders with various shapes and particle sizes have been successively synthesized by hydrothermal methods in a high alkaline medium with nitrate precursors. Chen et al. [13] synthesized single-phase BFO crystallites at temperatures as low as 200 °C with 4 M concentration of KOH. Xiaomeng et al. [14] synthesized submicrometer-sized BFO plates by a surfactant-assisted hydrothermal method at a temperature of 180 °C using cetyltrimethylammonium bromide (CTAB) as a surfactant.

* Corresponding author. Tel.: +82 41 540 5763; fax: +82 41 548 3502.
E-mail address: cicheon@hoseo.edu (C.I. Cheon).

0272-8842/$36.00
doi:10.1016/j.ceramint.2010.01.020

Han et al. [15] synthesized spindle-like BFO nanopowders at a temperature of 200 °C, adding a small amount of H_2O_2. Wang et al. [16] synthesized BFO nanoparticles with ~5 nm particle size by a mineralizer-assisted hydrothermal method at a temperature of 200 °C using KNO_3 as mineralizer. Cho et al. [17] synthesized spherical BFO nanopowders at a temperature of 130 °C with the aid of triethanolamine (TEA). While several studies have reported on the hydrothermal synthesis of BFO powders, only Chen et al. [13] have mentioned the phase formation mechanism of hydrothermal BFO powders. They reported that BFO powders could be obtained by a dissolution–precipitation mechanism, which entails the dissolution of bismuth and iron hydroxide by the attack of KOH and precipitation of insoluble powders from a super-saturated hydrothermal fluid [13]. Despite these advances in the understanding of hydrothermal synthesis of BFO powders, it is necessary to shed light on their chemical history in order to form final ceramic compositions and avoid second phase formation and control the particle size. Furthermore, the characteristics of these powders should be investigated to confirm that their quality will meet the demands of practical applications. In the current work, single-phase BFO powders were prepared at a temperature of roughly 200 °C by a hydrothermal method. The phase formation mechanism under various hydrothermal conditions was discussed. Typical characteristics including the magnetic property of the single-phase BFO powders were also investigated.

2. Experiment

The chemical reagents used in the work were bismuth nitrate ($Bi(NO_3)_3{\cdot}5H_2O$), iron nitrate ($Fe(NO_3)_3{\cdot}9H_2O$), and potassium hydroxide (KOH). All the chemicals were of analytical grade. Equi-molar mixtures of $Bi(NO_3)_3{\cdot}5H_2O$ and $Fe(NO_3)_3{\cdot}9H_2O$ were dissolved in 40 mL of KOH. The molar ratio of the alkali mineralizer was adjusted by dissolving certain amounts of KOH pellets into distilled water. The mixture was stirred vigorously for 30 min and transferred into a Teflon-lined stainless steel autoclave. Several modifications to the typical synthesis procedure were incorporated to study the effect of different synthesis conditions on phase formation and particle size. The concentration of KOH was varied from 4 to 12 M. The hydrothermal treatments were conducted under autogeneous pressure in a temperature range of 150–225 °C for 1–72 h. The produced powders were collected at the bottom of the Teflon-liner after cooling to room temperature. The products were washed at least five times by repeated cycles of centrifugation in distilled water, and redispersed in ethanol by sonicating for 30 min. Subsequently, powders were obtained by evaporating ethanol in a mortar heated at 80 °C.

The crystal structure and phase composition of the powders were determined using an X-ray diffractometer (XRD) (D/max-RC; Rigaku, Japan) with Cu Kα radiation operated at 30 kV and 60 mA in a 2θ range of 15–70°. The particle size and morphology were observed using field emission scanning electron microscopy (SEM) (XL30SFEG; Philips, Netherlands and S4300; HITACHI, Japan) equipped with an energy-dispersive X-ray (EDX) analysis unit. SEM samples were prepared as follows: BFO particles suspended in ethanol were sonicated and a few drops of the suspension were deposited onto a glass substrate, allowed to dry, and then sputter-coated with an osmium. Transmission electron microscopy (TEM) and selected area electron diffraction (SAED) images were taken with a Tecnai G2 F30 S-Twin (FEI, Netherlands) using an acceleration voltage of 300 kV to confirm single-crystalline behavior. TEM samples were prepared by sonicating BFO particles suspended in ethanol and dropping the suspension onto a 200 mesh carbon coated grid. Fourier transform infrared (FTIR) spectra of BFO powders were taken with a FTIR 4100 spectrometer (Jasco, Japan). Differential scanning calorimetry (DSC) (DSC 204 F1, NETZSCH, Germany) of BFO powders was performed from room temperature to 900 °C in argon ambient at a scan rate of 10 °C/min. The magnetic properties of the BFO powders were measured using a vibrating sample magnetometer (VSM) at room temperature.

3. Results

The influences of the different mineralizer concentrations, duration time, and reaction temperature on the phase formation of BFO powders were investigated under various hydrothermal conditions (as summarized in Table 1).

XRD patterns of the powders synthesized at 200 °C for 6 h using different KOH concentrations of 4, 8, and 12 M are presented in Fig. 1. The XRD pattern of the starting precursor powders dissolved in the KOH solution (hereafter ‘‘not reacted powder’’) shows only α-Bi_2O_3 phase. It was confirmed from XRD data of iron nitrate powders dissolved in KOH solution (results not shown) that iron ions exist in an amorphous hydroxide form in the KOH solution. Because the amorphous iron hydroxide has relatively broad- and low-intensity peaks than α-Bi_2O_3, the XRD pattern of the not reacted powder shows only α-Bi_2O_3 phase. With the 4 M concentration of KOH, crystalline BFO was obtained with an impurity phase of α-Bi_2O_3. Diffraction peaks of the BFO powders synthesized with 8 M KOH can be indexed to a pure BFO phase. With the higher

Table 1
The summary of hydrothermal synthetic conditions and phase structure of BFO powders.

KOH concentration (M)	Reaction temperature (°C)	Reaction time (h)	Phase structure
4	200	6	BFO, minor Bi_2O_3
8	200	6	Pure BFO
12	200	6	BFO, minor $Bi_{25}FeO_{40}$
8	200	1	Bi_2O_3
8	200	3	BFO, minor Bi_2O_3
8	200	24	BFO, minor $Bi_{25}FeO_{40}$ and Bi_2O_3
8	200	72	BFO, minor $Bi_{3.43}Fe_{0.57}O_6$ and Fe_2O_3
8	150	6	Bi_2O_3
8	175	6	Pure BFO
8	225	6	Pure BFO

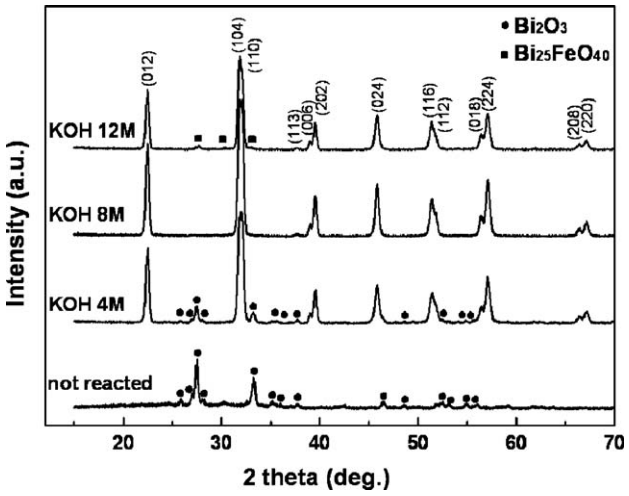

Fig. 1. XRD patterns of not reacted powder, BFO powders synthesized at 200 °C for 6 h with KOH concentration of 4, 8, and 12 M.

KOH concentration (12 M), an impurity phase of bismuth-rich $Bi_{25}FeO_{40}$ was detected in addition to the major BFO phase.

SEM images of the not reacted powder and BFO powders synthesized at 200 °C for 6 h using KOH concentrations of 4, 8, and 12 M are shown in Fig. 2. Energy-dispersive spectroscopy (EDS) spectra of the BFO powders synthesized with 4 M KOH are also shown. According to Figs. 1 and 2(a), α-Bi_2O_3 and amorphous iron hydroxide exhibit a fine, spherical structure with an average diameter of ∼30 nm. BFO phase was formed with a small amount of α-Bi_2O_3 phase when 4 M KOH was used as a mineralizer. Reaction products primarily consist of several hundred nanometer-sized plates with a broad particle size distribution and a small portion of nanorods with a high aspect ratio (Fig. 2(b)). EDS analyses confirm that the nanorods marked as "A" had contained bismuth and oxygen elements whereas the plates marked as "B" incorporated bismuth, iron, and oxygen elements with a Bi:Fe ratio of 1.14:1 within the instrumental accuracy, indicating that the nanorods are α-Bi_2O_3

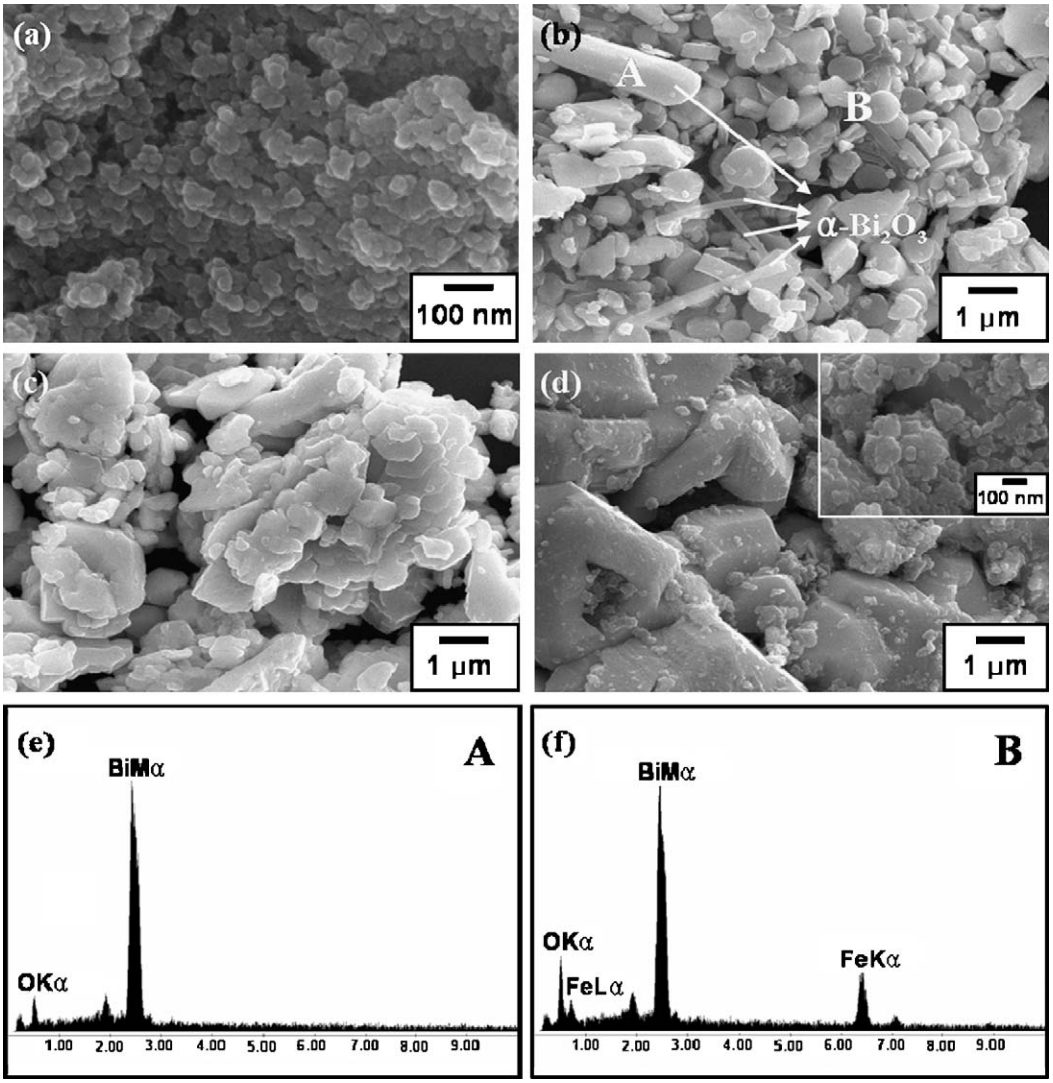

Fig. 2. SEM images of (a) not reacted powder, BFO powders synthesized at 200 °C for 6 h with KOH concentration of (b) 4 M, (c) 8 M, and (d) 12 M. The inset in (d) shows low magnification image of (d). (e and f) show EDX profile obtained from marked "A" and "B" in (b).

phase and the plates are BFO phase (Fig. 2(e) and (f)). The BFO powders synthesized with a KOH concentration of 8 M show soft agglomerates of irregular-shaped particles with several ten and/or hundred nanometers in size (Fig. 2(c)). In the case of BFO powders synthesized with 12 M KOH, several ten nanometer-sized spherical particles agglomerated to form several ten micrometer-sized aggregates (Fig. 2(d) and inset). With increasing KOH concentration, the particles became smaller and their morphology changed from plate- to spherical-like, and they were more agglomerated, as shown Fig. 2(b–d).

XRD patterns and SEM images obtained from powders reacted for times ranging from 1 to 72 h at 200 °C with 8 M KOH are shown in Figs. 3 and 4, respectively. The not reacted powder and the powders synthesized for 1 h were equally indexed as α-Bi_2O_3 phase but the peak intensity of the powder synthesized for 1 h was relatively increased. The powder synthesized for 1 h consisted of rod-like particles and spherical nanoparticles of various sizes, as shown in Fig. 4(a). EDX analyses confirm that the Bi:Fe ratio in the rod-like particles

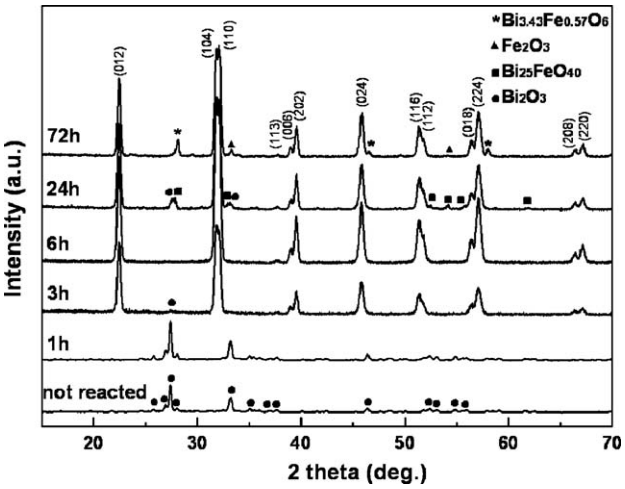

Fig. 3. XRD patterns of not reacted powder, BFO powders synthesized at 200 °C with 8 M KOH concentration for various reaction times of 1–72 h.

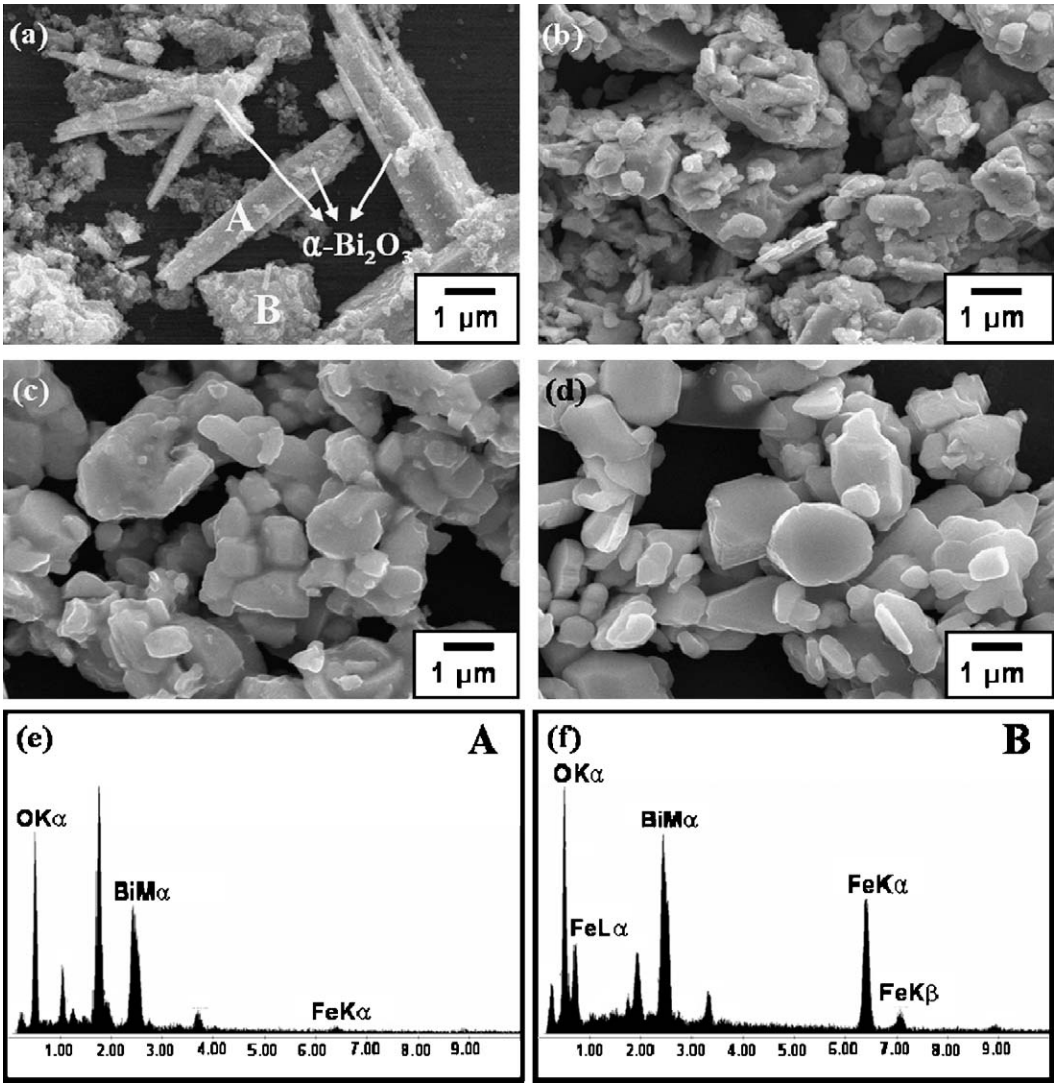

Fig. 4. SEM images of BFO powders synthesized at 200 °C with 8 M KOH concentration for various reaction times of (a) 1 h, (b) 3 h, (c) 24 h, and (d) 72 h. (e and f) show EDX profile obtained from marked "A" and "B" in (a).

was 7.15:1 whereas the ratio was 0.36:1 in the spherical nanoparticles, within the instrumental accuracy. It can be concluded that the rod-like particles are α-Bi_2O_3 phase, similar to the nanorods synthesized with 4 M KOH (Figs. 1 and 2(b)). The small amount of iron element might have originated from the spherical nanoparticles adhered on the rod-like particles, as shown in Fig. 4(a). The peaks excluding the bismuth, iron, and oxygen peaks shown in the EDS spectra of Fig. 4(e and f) originate from the glass substrate and the conductive coating material (osmium) for SEM observation. The phase transformation from α-Bi_2O_3 with amorphous hydroxide to BFO was initiated between 1 and 3 h, and α-Bi_2O_3 phase was completely eliminated after 6 h. Meanwhile, the presence of second phases such as α-Bi_2O_3, $Bi_{25}FeO_{40}$, Fe_2O_3, and $Bi_{3.43}Fe_{0.57}O_6$ was detected in addition to the major BFO phase for the powders synthesized for 24 and 72 h. SEM images of the BFO powders show that several ten nanometer-sized spherical BFO particles were initially formed (3 h), and subsequently developed into several hundred nanometer-sized and/or several micrometer-sized particles with plate- and polyhedral-like morphologies (Fig. 4(b), Fig. 2(c), Fig. 4(c) and (d)).

Fig. 5 shows XRD patterns of the powders synthesized at 150, 175, 200, and 225 °C for 6 h with a KOH concentration of 8 M. The XRD pattern of the not reacted powder is also included in the figure. It can be seen that pure BFO powders were obtained at a temperature of ≥175 °C. The powder synthesized at 150 °C had the same XRD peak position and similar peak intensity with the not reacted powders, in which α-Bi_2O_3 and amorphous hydroxide were detected. The morphology of the particles was also similar (Fig. 6(a)). The change in

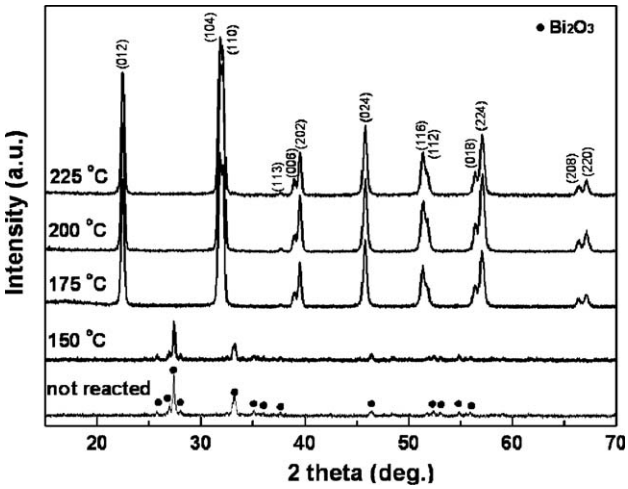

Fig. 5. XRD patterns of not reacted powder, BFO powders synthesized with 8 M KOH concentration for 6 h at various reaction temperatures of 150–225 °C.

the particle morphology with the reaction temperature (Fig. 6) follows a similar trend to the duration time (Fig. 4). That is, the particle morphology changed from several ten nanometer-sized spherical particles to several hundred nanometer-sized and/or several micrometer-sized particles with plate- and polyhedral-like shape as the reaction temperature was increased from 150 to 225 °C (Fig. 6(a, b), Fig. 2(c), Fig. 6(c)).

Characteristics of the single-phase BFO powder synthesized at 200 °C for 6 h under a KOH concentration of 8 M were investigated in detail. A representative TEM image of the single-phase BFO particles is shown in Fig. 7(a). SAED data

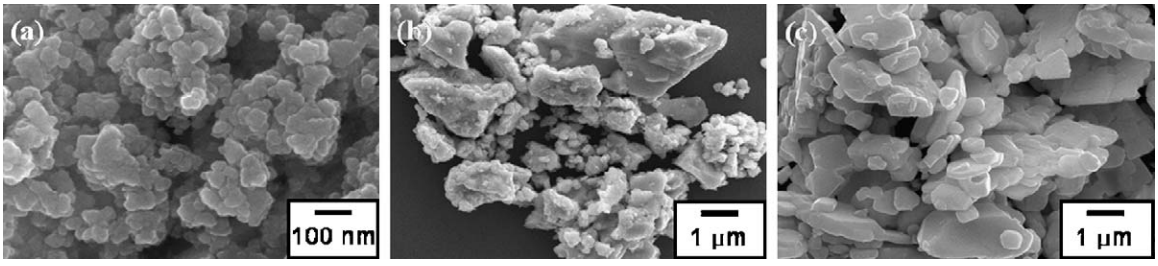

Fig. 6. SEM images of (a) not reacted powder, BFO powders synthesized with KOH concentration of 8 M for 6 h at reaction temperature of (b) 175 °C, and (c) 225 °C.

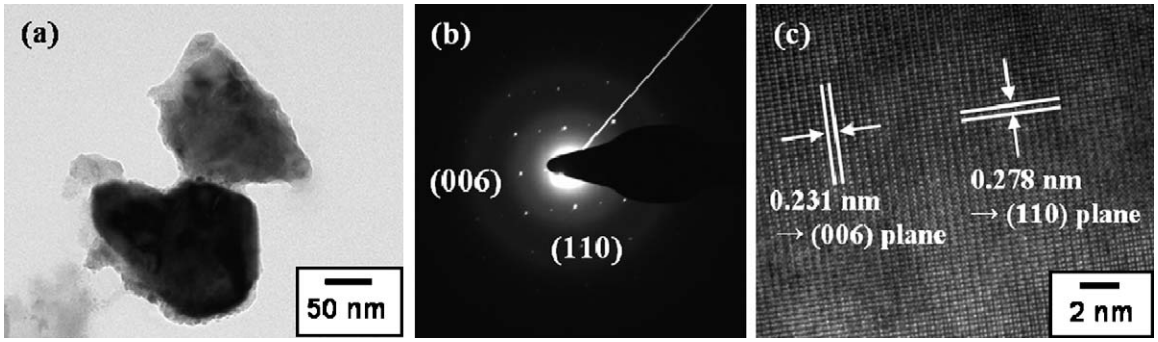

Fig. 7. (a) Low resolution TEM image, (b) SAED pattern, and (c) high-resolution TEM image of BFO powders synthesized with 8 M KOH concentration for 6 h at 200 °C.

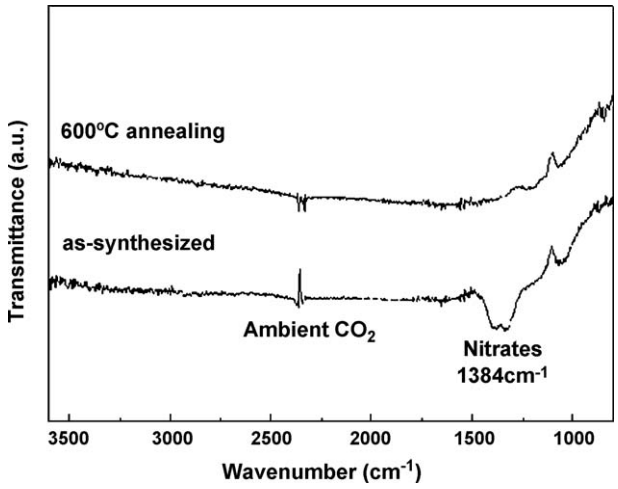

Fig. 8. FTIR spectra of BFO powders synthesized with 8 M KOH concentration for 6 h at 200 °C: (a) as-synthesized and (b) annealed at 600 °C.

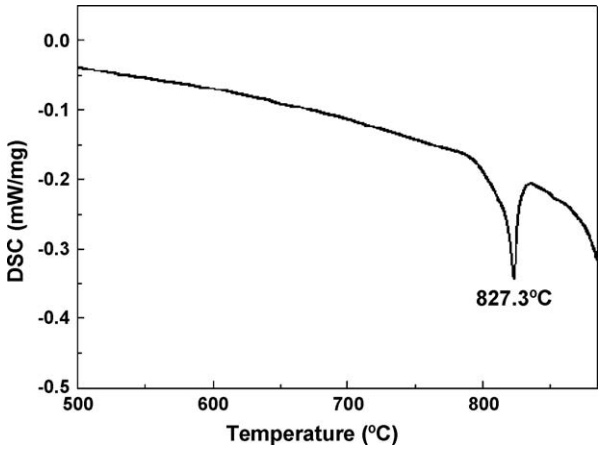

Fig. 9. DSC curve of the BFO powders synthesized with 8 M KOH concentration for 6 h at 200 °C.

taken from an individual particle shows the presence of sharp diffraction spots, which are indicative of single-crystalline BFO formation (Fig. 7(b)). In Fig. 7(c), a high-resolution TEM image obtained from a portion of an individual BFO particle is shown for further confirmation of the single-crystalline behavior of the BFO powder. This image shows a clearly resolved crystalline domain with uniform interplanar spacings of 2.78 and 2.31 Å, which are compatible with the bulk BFO values of 2.79 and 2.31 Å, respectively (JCPDS card no. 86-1518). The lattice spacings described above correspond to the (1 1 0) and (0 0 6) planes of a rhombohedral phase BFO crystal. The FTIR spectrum of the single-phase BFO powder presented in Fig. 8 indicates that neither lattice water nor hydroxide species were present. This is assumed from the lack of characteristic absorption bands in the regions of 3550–3200 and 1630–1600 cm^{-1} corresponding to antisymmetric and symmetric OH stretching and HOH bending, respectively [18]. The band at 1384 cm^{-1} corresponds to the nitrate peak [19], which was eliminated after annealing at 600 °C. The DSC curve shown in Fig. 9 reveals an endothermic peak at 827.3 °C.

Fig. 10 shows the magnetization curve measured at room temperature for the single-phase BFO powders. A partly enlarged view of Fig. 10 is shown in the inset over a low H region. The curve shows weak ferromagnetism at room temperature with a remanent magnetization value (M_r) of approximately 5.66 memu/g and a coercive field value (H_c) of nearly 160 Oe.

4. Discussion

It was confirmed that the not reacted powder consisted of α-Bi_2O_3 and amorphous iron hydroxide nanoparticles with a spherical shape. The α-Bi_2O_3 and amorphous iron hydroxide phase was immediately induced from the dissolved $Bi(NO_3)_3$ and $Fe(NO_3)_3$ precursor powders in the KOH solution according to the follow reaction:

$$2Bi(NO_3)_3 + 6KOH \rightarrow Bi_2O_3 + 6K^+ + 6NO_3^- + 3H_2O$$

$$Fe(NO_3)_3 + 3KOH \rightarrow Fe(OH)_3 + 3K^+ + 3NO_3^-$$

With a low concentration of KOH (4 M), the α-Bi_2O_3 phase was still shown in addition to the major BFO phase in the form of nanorods, as shown in Fig. 2(b). With a higher concentration of KOH (8 M), α-Bi_2O_3 nanorods disappeared, indicating that the α-Bi_2O_3 phase was dissolved by a higher concentration of alkali mineralizer. This phenomenon was also observed for the powders synthesized at 200 °C with an 8 M KOH concentration for 1–6 h. The α-Bi_2O_3 phase transformed into rod-like particles with increased crystallinity after synthesizing for 1 h and was eliminated after 6 h. Yang et al. [20] synthesized α-Bi_2O_3

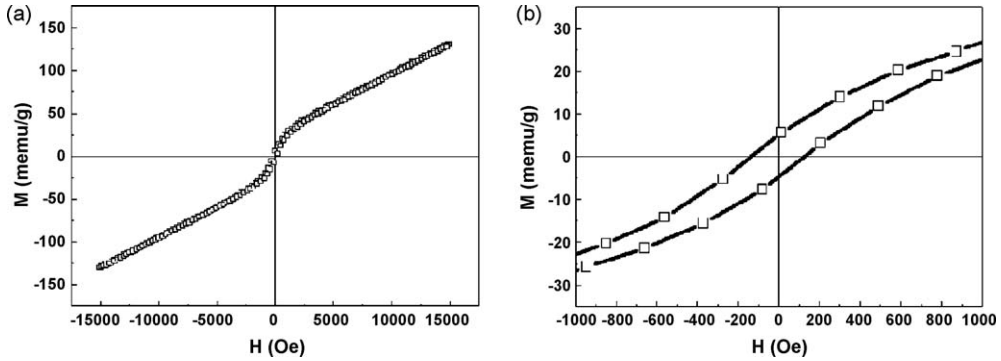

Fig. 10. (a) VSM measurement of BFO powders synthesized with 8 M KOH concentration for 6 h at 200 °C, and (b) the partially enlarged curve of (a).

needles by hydrothermal synthesis using a $Bi(OH)_3$ precursor in a 0.5 M KOH mineralizer at 120 °C. These results show preferential growth of α-Bi_2O_3 phase with a rod-like morphology in a hydrothermal system using a low concentration of alkaline mineralizer at low temperature. It can be conjectured that spherical α-Bi_2O_3 nanoparticles formed at room temperature transform into α-Bi_2O_3 rod-like particles with a high aspect ratio at the initial stage of hydrothermal synthesis. As the concentration of the KOH mineralizer and/or duration time increase, rod-like α-Bi_2O_3 particles gradually dissolve into Bi^{3+} ions. The chemical reaction of phase transformation from α-Bi_2O_3 with amorphous hydroxide into $BiFeO_3$ is as follows:

$$Bi_2O_3 + 2Fe(OH)_3 \rightarrow 2BiFeO_3 + 3H_2O$$

Increasing the reaction temperature also enhances the dissolution rate of α-Bi_2O_3 phase. In spite of a small variation of temperature from 150 to 175 °C, the phase was totally changed from α-Bi_2O_3 to pure BFO, indicating the dissolution of α-Bi_2O_3 and that nucleation of BFO occurs dramatically within this narrow temperature range.

The effects of processing parameters on the BFO phase formation may be understood by a dissolution–precipitation mechanism [13,21,22]. Further increasing of pH, duration time, and reaction temperature after the formation of α-Bi_2O_3 rod-like particles increase α-Bi_2O_3 solubility, thereby increasing the dissolution rate of bismuth into solution and increasing the ion concentration in the alkaline solution. When the ion concentration in the alkaline solution surpasses the saturation point, thermodynamically stable BFO phase can be nucleated and grown. However, BFO phase formation can start before the rod-like α-Bi_2O_3 particles completely dissolve in the solution during a certain period of hydrothermal synthesis when the Bi ion concentration in the solution exceeds the saturation point. This phenomenon can be confirmed from the coexistence of α-Bi_2O_3 and BFO phases in the powders synthesized at 200 °C for 6 h with 4 M KOH (Figs. 1 and 2(b)) and at 200 °C with 8 M KOH for 3 h (Figs. 3 and 4(b)). As continuous dissolution of α-Bi_2O_3 and precipitation of BFO lead to a long period of nucleation, the particles nucleated at the early stage of precipitation grow larger than those nucleated later. This might be the origin of the broad particle size distribution shown in Figs. 2(b, c), 4, and 6. Further growth of BFO particles was still possible after the formation of BFO phase by the dissolution of small BFO particles and precipitation on large particles. Through a repeated dissolution–precipitation process, which is called Ostwald-ripening, BFO particles grew larger to minimize the surface energy as the duration time was increased (Figs. 2(c), 4(b, c, and d)).

On the other hand, the nucleation and growth rate depend on the degree of super-saturation in the solution; there is a high nucleation rate and low growth rate at high super-saturation, while a low nucleation rate and high growth rate will occur at low super-saturation. The high degree of super-saturation in the solution with the high KOH concentration results in a high nucleation rate for the BFO phase. This explain the decrease of the particle size with increasing KOH concentration, as shown in Fig. 2(b–d), and in particular, accounts for the spherical BFO nanoparticles with several nanometer size in the 12 M KOH solution. In the higher KOH concentration, the base OH^- ions might act as a bridge between particles, and thus BFO powders synthesized with 12 M KOH tended to strongly agglomerate.

After the formation and growth of BFO phase by the reaction between bismuth and iron, the concentration of bismuth, iron, and OH^- in the hydrothermal solution becomes small. Because thermodynamic states such as source ion concentration and pH value were changed compared with the initial BFO formation conditions, a second phase might be formed as the reaction time was prolonged (Fig. 3). The minor phase of $Bi_{25}FeO_{40}$ that formed with the BFO powders at 12 M KOH, which is presented in Fig. 1, also might arise from different thermodynamic states originating from larger solubility of α-Bi_2O_3 phase and higher pH value.

Increasing the reaction temperature with a constant concentration of alkali mineralizer and duration time (8 M KOH, 6 h) did not influence the phase formation and only resulted in an increase of particle size (Fig. 5). Rossetti et al. [21] demonstrated that the rate of dissolution and crystallization were strongly dependent on the reaction temperature, which means the reaction temperature is related to the kinetics of the particle formation process. Consequently, the reaction temperature only influences the duration time to crystallize the BFO phase and does not influence the formation of different phases when other experimental conditions are unchanged. Chen et al. [13] obtained pure-phase BFO powders above the critical temperature of ∼200 °C and observed an increase of particle size with increased reaction temperature, which is consistent with our experimental results.

From the TEM analyses, we confirmed the single-crystalline behavior of the single-phase BFO powders. Although the conditions under which single-phase BFO powders can be obtained are narrow, BFO powders synthesized by a hydrothermal method have good crystallinity. Surface H_2O and OH^- defects are detrimental to the electrical properties of inorganic materials [23]. The FTIR results showed neither lattice water nor hydroxide species, indicating that the BFO powders fabricated by the hydrothermal method have fewer defects and impurities in the lattice. The endothermic peak at 827.3 °C from the DSC curve resulted from a ferroelectric to paraelectric phase transformation in BFO, which is in good agreement with the previous reports [24].

The weak ferromagnetic property shown in Fig. 10 is different from the linear *M–H* behavior noted in bulk BFO [25]. Park et al. [12] suggested that incomplete spin compensation is possible in a small antiferromagnetic system below the wavelength period of the spiral spin arrangement of 62 nm, where the long-range antiferromagnetic order is frequently interrupted at the particle surfaces. In small structures, the surface-to-volume ratio becomes very large with decreasing particle size, enhancing the contribution to the overall magnetization by uncompensated spins at the surface [12]. Our BFO powders with a particle size of several ten and/or hundred nanometers have a comparable magnetization value with that of the 95 nm-sized BFO particles from Ref. [12]. In addition to the contribution of particle size effects to the

magnetization value, canting or incomplete counterbalance of the antiferromagnetic spin structure due to structural distortion induces increased magnetization [26,27].

5. Conclusion

In the present study, the influence of processing variables such as KOH concentration, duration time, and reaction temperature on the phase formation and particle size of BFO powders synthesized by a hydrothermal method was investigated. The optimum conditions to retain pure-phase BFO were determined to be a KOH concentration of 8 M for a reaction time of 6 h at 175–225 °C. A dissolution–precipitation process was discussed as the hydrothermal mechanism to form BFO crystallites. BFO particle growth was promoted by lowering the KOH concentration, or increasing duration time or reaction temperature. Weak ferromagnetic behavior observed from the single-phase BFO powder might be originated from particle size effect and canting of the antiferromagnetic spin structure.

Acknowledgement

This research was financially supported by a grant from the Fundamental R&D Program for Core Technology of Materials funded by the Ministry of Knowledge Economy, Republic of Korea.

References

[1] H. Schmid, Multi-ferroic magnetoelectrics, Ferroelectrics 162 (1994) 317–338.
[2] N. Hur, S. Park, P.A. Sharma, J.S. Ahn, S. Guha, S.-W. Cheong, Electric polarization reversal and memory in a multiferroic material induced by magnetic fields, Nature 429 (2004) 392–395.
[3] W. Eerenstein, N.D. Mathur, J.F. Scott, Multiferroic and magnetoelectric materials, Nature 442 (2006) 759–765.
[4] G.A. Smolenskii, I.E. Chupis, Ferroelectromagnets, Sov. Phys. Usp. 25 (1982) 475–493.
[5] I.G. Ismailzade, X-Ray diffractometric determination of the Curie temperature and temperature dependence of spontaneous polarization of hexagonal (rhombohedral) ferroelectrics, Phys. Status Solidi B 46 (1971) K39–K41.
[6] K. Takahashi, N. Kida, M. Tonouchi, Terahertz radiation by an ultrafast spontaneous polarization modulation of multiferroic $BiFeO_3$ thin films, Phys. Rev. Lett. 96 (2006) 117402.
[7] R.F. Taylor, J.S. Schultz, Handbook of Chemical and Biological Sensors, Institute of Physics Pub., Bristol and Philadelphia, 1996, pp. 376.
[8] G.D. Achenbach, W.J. James, R. Gerson, Preparation of single-phase polycrystalline $BiFeO_3$, J. Am. Ceram. Soc. 50 (1967) 437.
[9] Y.P. Wang, L. Zhou, M.F. Zhang, X.Y. Chen, J.-M. Liu, Z.G. Liu, Room-temperature saturated ferroelectric polarization in $BiFeO_3$ ceramics synthesized by rapid liquid phase sintering, Appl. Phys. Lett. 84 (2004) 1731–1733.
[10] A.K. Pradhan, K. Zhang, D. Hunter, J.B. Dadson, G.B. Loutts, P. Bhattacharya, R. Katiyar, J. Zhang, D.J. Sellmyer, Magnetic and electrical properties of single-phase multiferroic $BiFeO_3$, J. Appl. Phys. 97 (2005) 093903.
[11] S. Ghosh, S. Dasgupta, A. Sen, H.S. Maiti, Low-temperature synthesis of nanosized bismuth ferrite by soft chemical route, J. Am. Ceram. Soc. 88 (2005) 1349–1352.
[12] T.J. Park, G.C. Papaefthymiou, A.J. Viescas, A.R. Moodenbaugh, S.S. Wong, Size-dependent magnetic properties of single-crystalline multiferroic $BiFeO_3$ nanoparticles, Nano Lett. 7 (2007) 766–772.
[13] C. Chen, J. Cheng, S. Yu, L. Che, Z. Meng, Hydrothermal synthesis of perovskite bismuth ferrite crystallites, J. Cryst. Growth 291 (2006) 135–139.
[14] L. Xiaomeng, X. Jimin, S. Yuanzhi, L. Jiamin, Surfactant-assisted hydrothermal preparation of submicrometer-sized two-dimensional $BiFeO_3$ plates and their photocatalytic activity, J. Mater. Sci. 42 (2007) 6824–6827.
[15] J.T. Han, Y.H. Huang, X.J. Wu, C.L. Wu, W. Wei, B. Peng, W. Huang, J.B. Goodenough, Tunable synthesis of bismuth ferrites with various morphologies, Adv. Mater. 18 (2006) 2145–2148.
[16] Y. Wang, G. Xu, Z. Ren, X. Wei, W. Weng, P. Du, G. Shen, G. Han, Mineralizer-assisted hydrothermal synthesis and characterization of $BiFeO_3$ nanoparticles, J. Am. Ceram. Soc. 90 (2007) 2615–2617.
[17] C.M. Cho, J.H. Noh, I.-S. Cho, J.-S. An, K.S. Hong, J.Y. Kim, Low-temperature hydrothermal synthesis of pure $BiFeO_3$ nanopowders using triethanolamine and their applications as visible-light photocatalysts, J. Am. Ceram. Soc. 91 (2008) 3753–3755.
[18] K. Nakamoto, Infrared and Raman Spectra of Inorganic and Coordination Compounds, John Wiley & Sons, New York, 1997, p. 70, 75.
[19] I. Nakagawa, J.L. Walter, Optically active crystal vibrations of the alkali-metal nitrates, J. Chem. Phys. 51 (1969) 1389–1397.
[20] Q. Yang, Y. Yin, Q. Li, P. Wang, Y.B. Cheng, Hydrothermal synthesis of bismuth oxide needles, Mater. Lett. 55 (2002) 46–49.
[21] G.A. Rossetti Jr., D.J. Watson, R.E. Newnham, J.H. Adair, Kinetics of the hydrothermal crystallization of the perovskite lead titanate, J. Cryst. Growth 116 (1992) 251–259.
[22] C.R. Peterson, E.B. Slamovich, Effect of processing parameters on the morphology of hydrothermally derived $PbTiO_3$ powders, J. Am. Ceram. Soc. 82 (1999) 1702–1710.
[23] A.T. Chien, X. Xu, J.H. Kim, J. Sachleben, J.S. Speck, F.F. Lange, Electrical characterization of $BaTiO_3$ heteroepitaxial thin films by hydrothermal synthesis, J. Mater. Res. 14 (1999) 3330–3339.
[24] J.R. Teague, R. Gerson, W.J. James, Dielectric hysteresis in single crystal $BiFeO_3$, Solid State Commun. 8 (1970) 1073–1074.
[25] S.T. Zhang, M.H. Lu, D. Wu, Y.F. Chen, N.B. Ming, Larger polarization and weak ferromagnetism in quenched $BiFeO_3$ ceramics with a distorted rhombohedral crystal structure, Appl. Phys. Lett. 87 (2005) 262907.
[26] M.M. Kumar, S. Srinath, G.S. Kumar, S.V. Suryanarayana, Spontaneous magnetic moment in $BiFeO_3$-$BaTiO_3$ solid solutions at low temperatures, J. Magn. Magn. Mater. 188 (1998) 203–212.
[27] S. H. Han, K. S. Kim, H. G. Kim, H.-G. Lee, H.-W. Kang, C. I. Cheon, J. S. Kim, Crystal structure and spontaneous magnetism of $BiFeO_3$ powder synthesized by hydrothermal method, J. Nanosci. Nanotechnol. In press.